Supporting Information

Flexible graphite films with high cross-plane thermal conductivity prepared by graphitization of polyimide catalyzed by Ni-coated-CNTs

Shuaizhen Li, Zhibo Zheng, Siwei Liu, Zhenguo Chi, Yi Zhang*, Jiarui Xu*

PCFM Lab, GD HPPC Lab, Guangdong Engineering Technology Research Centre for High-performance Organic and Polymer Photoelectric Functional Films, State Key Laboratory of Optoelectronic Materials and Technologies, School of Chemistry, Sun Yat-sen University, Guangzhou 510275, China.

E-mail: liusiw@mail.sysu.edu.cn (Siwei Liu); ceszy@mail.sysu.edu.cn (Yi Zhang);

Measurements and characterization

The crystalline structure of graphitized films was characterized using X-ray diffraction (XRD, Bruker D8) with Cu-K_a radiation (λ = 1.54051 A)._The scanning speed is 5 °/min, and the scanning range is 5~80 °.

According to the Bragg's equation (Equation (1)), the average interlayer spacing of d_{002} can be obtained.

$$\lambda=2d\sin\theta \quad (1)$$

According to the Mering-Maire empirical formula, the graphitization degree of graphite films can be calculated by Equation (2):

$$G=(0.344-d_{002})/(0.344-0.3354) *100\% \quad (2)$$

Herein, the average interlayer spacing of the ideal graphite crystal is 0.3354 nm, and the average interlayer spacing of amorphous carbon is 0.3440 nm.

The cross-section morphologies of the graphitized films were observed by a Japan Hitachi S4800 Field emission scanning electron microscopy (FE-SEM) with an

accelerating voltage of 10 KV.

The interior structures of the graphitized films were observed by a Spherical Aberration-Corrected High Resolution Electron Microscopy (JEM-ARM200F, Japan) with an accelerating voltage of 200 kV.

Raman spectra of the graphitized films were measured using a Raman spectrometer (LabRam HR800, Horiba Jobin Yvon Inc.) with a laser operating at a wavelength of 532 nm as the excitation source. The degree of graphitization can be represented by the *R* value, which is calculated by the formula $R=I_D/I_G$. The smaller the *R* value, the higher the degree of graphitization.

The thermal diffusivity (α, $mm^2 \cdot s^{-1}$) at room temperature was measured on disk samples via the laser flash method (Netzsch Instruments Co., Nanoflash LFA 447 system), the test samples were cut into round slice with a diameter of 25 mm for the in-plane thermal diffusivity test and 12.5 mm for the cross-plane thermal diffusivity test. The thickness of all the samples was 35 μm. The specific heat (C_p, $J \cdot g^{-1} \cdot K^{-1}$) at room temperature was measured on disk samples via differential scanning calorimetry (DSC, Perkin-Elmer Co., DSC-8500), and the bulk density (ρ, $g \cdot cm^{-3}$) of the specimens was measured via the water displacement method (Alfa Mirage Co. Ltd, Electronic Densimeter SD-200L). For each measurement, five samples were tested three times. The thermal conductivity (λ, $W \cdot m^{-1} \cdot K^{-1}$) was calculated using the following equation: $\lambda=C_p \cdot \rho \cdot \alpha$. The electric conductivities of the graphite films were measured with a four-probe resistance tester.

Bending property of graphite film were tested by three-point bending method using WNLS-200 Electronic Universal Materials Testing System. The measurement was carried out with a 20 mm span and a cross head speed of 30 mm/min in circulation model of 5 circles. The bending strength, σ_b, were calculated according to following Equation (3):

$$\sigma_b = \frac{3FL}{2WT^2} \tag{3}$$

Where *F* is the maximum load value (*N*), *L* is the span (mm), *W* is the sample width (mm) and *T* is the sample thickness (mm).

Table S1 the formulation of nickel chemical plating solution

Compound	Concentration ($g \cdot L^{-1}$)
Nickel sulfate hexahydrate	30
Sodium hypophosphite hydrate	18
Trisodium citrate dihydrate	6
ammonium chloride	72

Note: the plating solution was prepared at room temperature and adjusted to pH=9.2 with ammonia.

Table S2. Thermal conductive data of the graphite films

sample	$\alpha_{//}$ ($m \cdot s^{-1}$)	$\alpha_{\perp}$ ($m \cdot s^{-1}$)	C_p ($J \cdot g^{-1}K^{-1}$)	ρ ($g \cdot mL^{-1}$)	$\lambda_{//}$ ($W \cdot m^{-1} \cdot K^{-1}$)	$\lambda_{\perp}$ ($W \cdot m^{-1} \cdot K^{-1}$)
G0	920.1	1.623	0.74	1.76	1198.4±0.2	2.11±0.05
G0.4	820.2	3.776	0.75	2.21	1359.5±0.2	6.26±0.05
G0.6	769.1	4.216	0.73	2.14	1201.5±0.2	6.59±0.05
G0.8	688.3	5.107	0.73	2.11	1060.2±0.2	7.87±0.05
G1	620.6	7.328	0.74	2.08	955.2±0.2	11.28±0.05

When the graphitization temperature is further increased from 2100 to 2800 ℃, the d_{002} space decreases from 0.3377 to 0.3354 nm, which is closer to the average interlayer spacing of the ideal graphite crystal (0.3354 nm). These results show that the pyrolysis temperature is still the main factor affecting the graphitization degree.

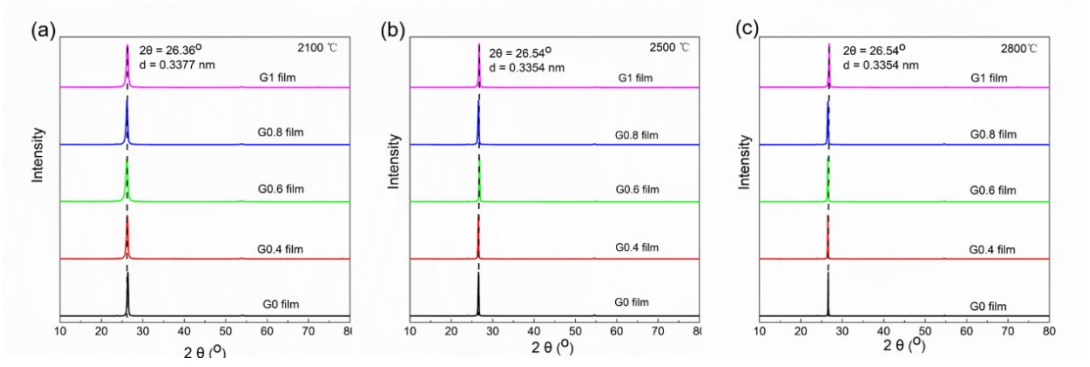

Figure S1 XRD pattern of graphite films at different graphitization temperature (a)

2100℃; (b) 2500 ℃; (c) 2800 ℃.

For the graphitization degree of the cross section, the addition of Ni@CNTs shows remarkable effect on improving the graphitization degree. The ID/IG (cross section) values of G0.4 film are obviously lower than that of G0 film at each graphitization temperature. These results indicated that the addition of Ni@CNTs was beneficial to improve of the overall graphitization degree of the graphite films.

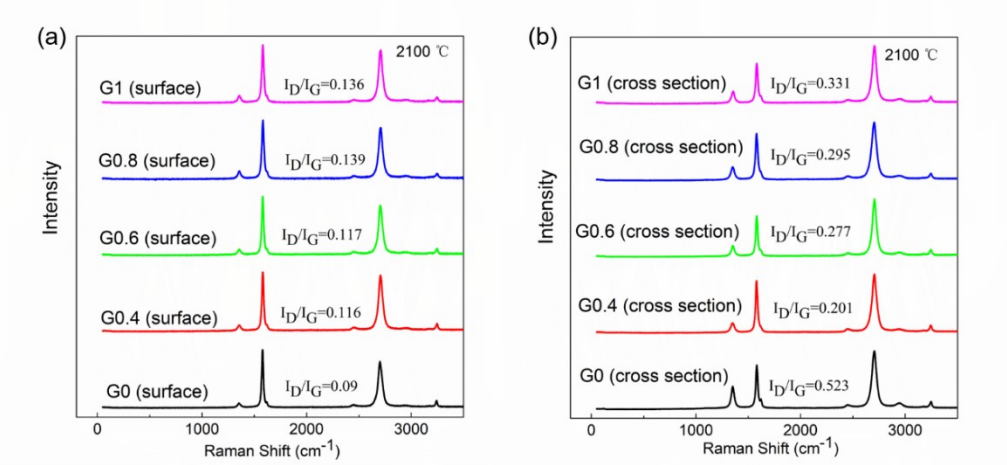

Figure S2 Raman spectrum of (a) surface and (b) cross section of graphite film at 2100 ℃.

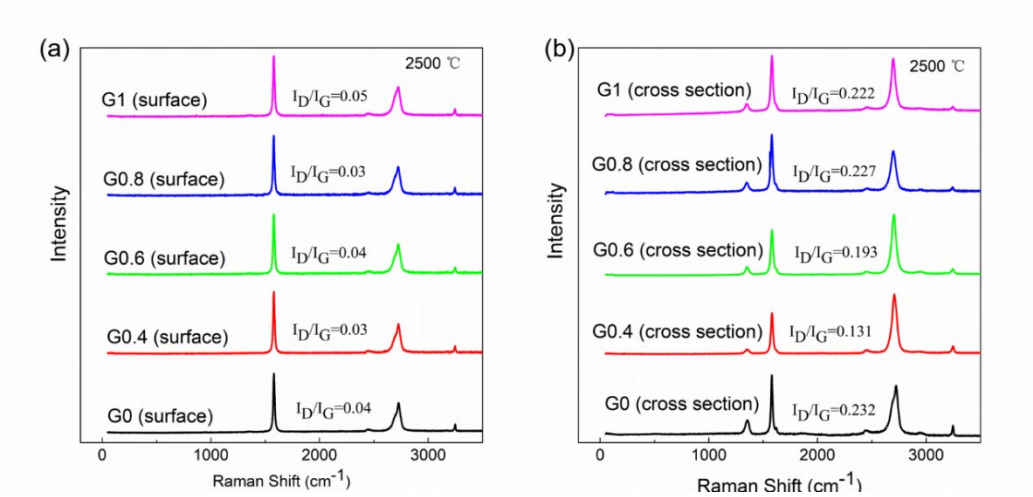

Figure S3 Raman spectrum of (a) surface and (b) cross section of graphite film at 2500 ℃.

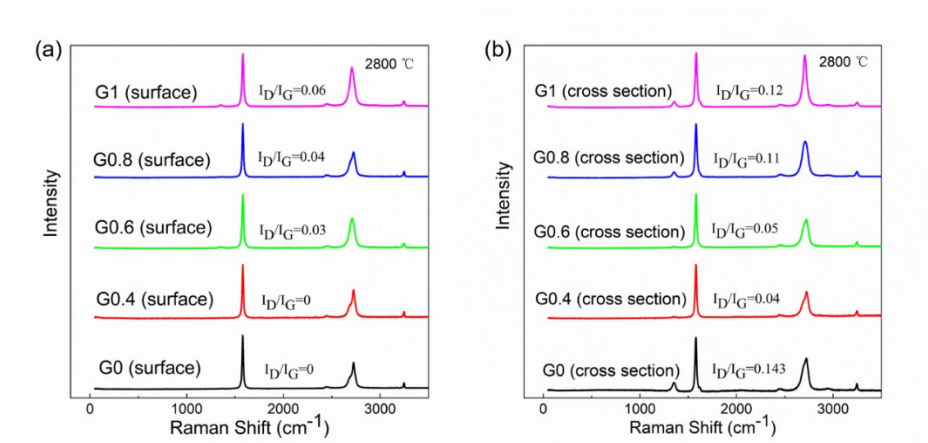

Figure S4 Raman spectrum of (a) surface and (b) cross section of graphite film at 2800 ℃.

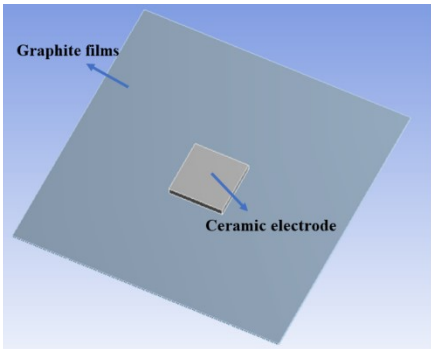

Figure S5 FES model (Modeling by Pro-E).

Both P0 and P0.4 film show an obvious and regular layer-by-layer structure, which is the prerequisite for obtaining high-quality graphite film. In contrast to P0 film, some carbon nanotubes crossing through P0.4 film can be seen in the SEM image, which can enhance the cross-plane thermal conductivity.

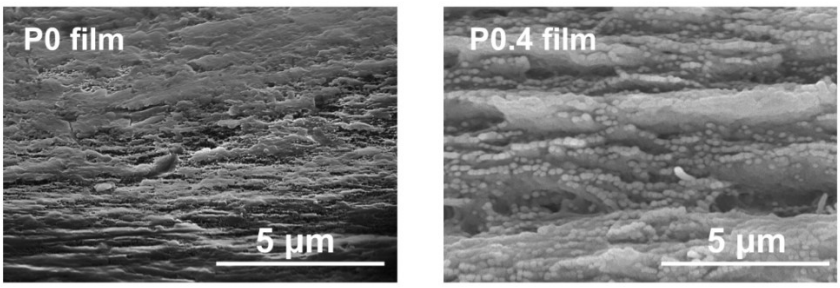

Figure S6 SEM images of cross-section of P0 film and P0.4 film.

The XRD patterns result **(Figure S7)** indicates that the addition of Ni@CNTs can

slightly increase the intersegmental distance of PI film. In addition, the storage modulus and glass transition temperature also increase with the addition of Ni@CNTs **(Figure S8)**.

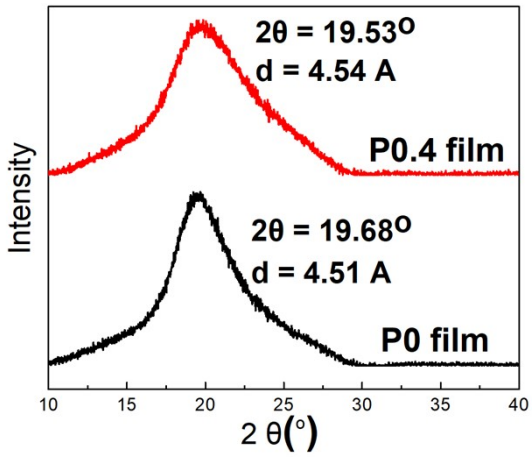

Figure S7 XRD pattern of P0 film and P0.4 film.

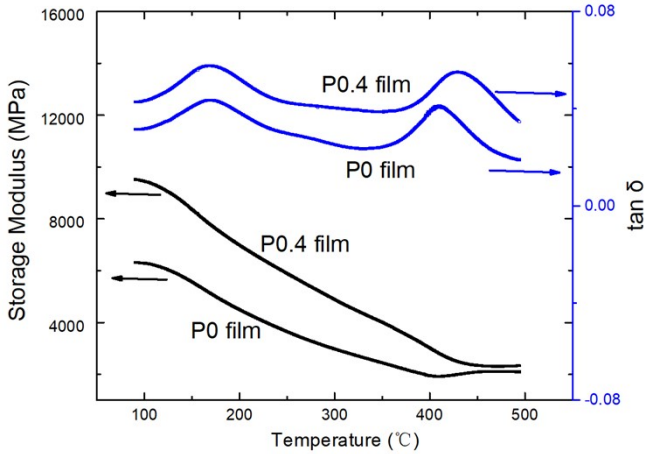

Figure S8 DMA curve of P0 film and P0.4 film.

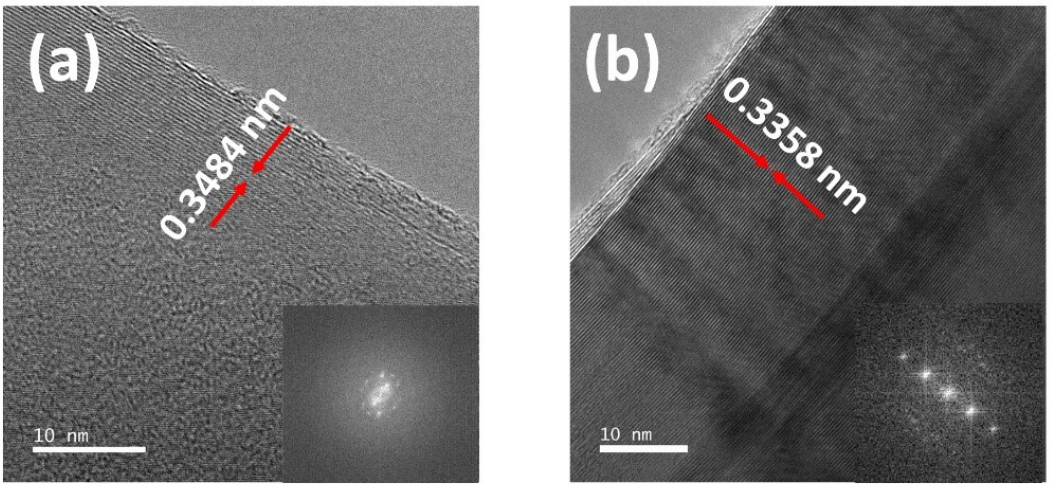

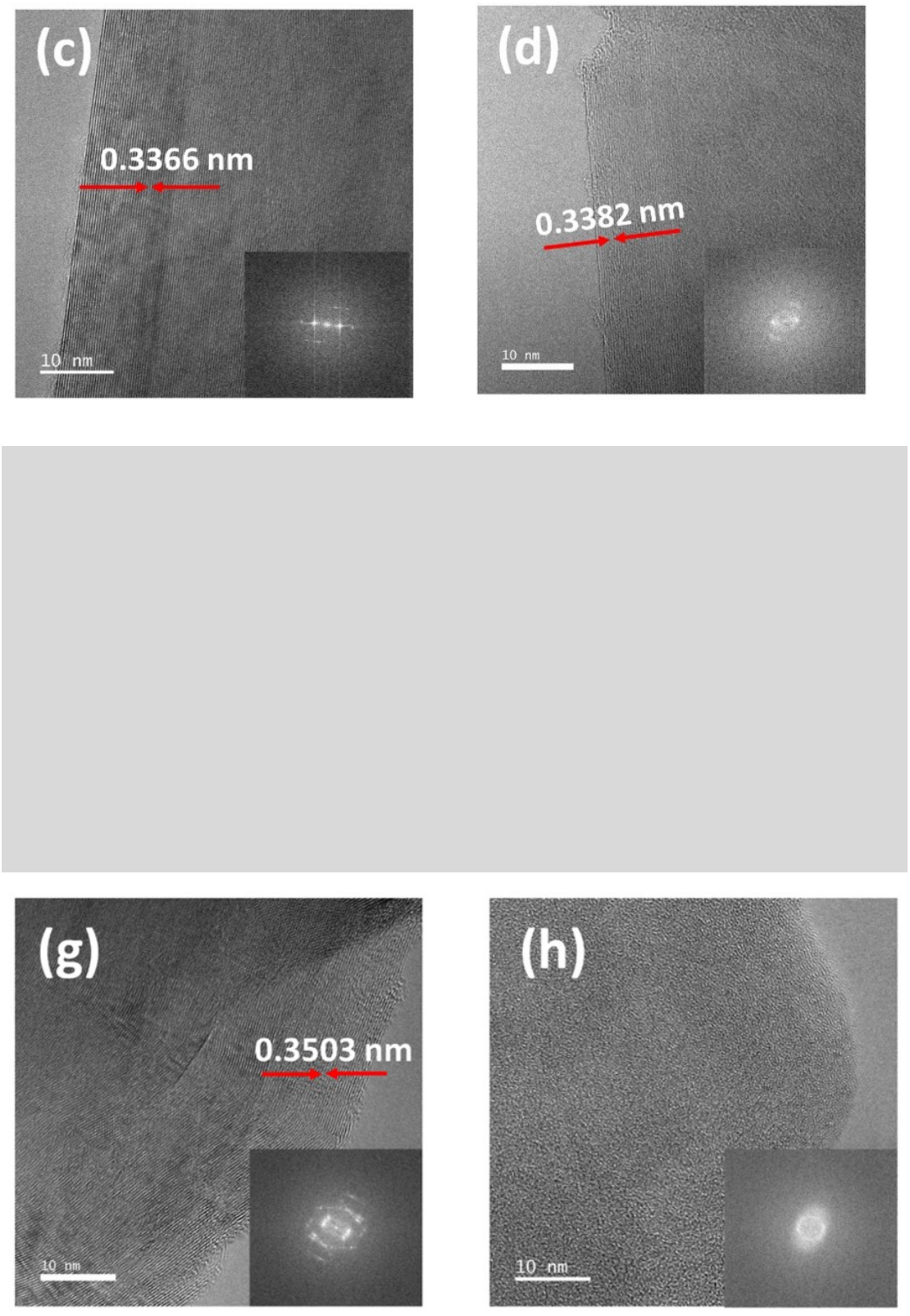

Figure S9 TEM images of graphite films (a) G0 film graphitized at 2800 ℃; (b) G0.4 film graphitized at 2800 ℃; (c) G0.6 film graphitized at 2800 ℃; (d) G0.8 film graphitized at 2800 ℃; (e) G1 film graphitized at 2800 ℃; (f) G0.4 film graphitized at 2500 ℃ (The graphite layer

spacing of the G0.4 film enlarged to 0.3416 nm); (g) G0.4 film graphitized at 2100 ℃ (The graphite layer spacing of the G0.4 film enlarged to 0.3503 nm); (h) C0.4 film carbonized at 1300 ℃ (amorphous).